

On enhanced descend algorithms for solving frictional multi-contact problems : applications to the Discrete Element Method

Serge Dumont¹

March 3, 2013

¹ LAMFA, Université de Picardie Jules Verne - CNRS UMR 7352, 33, rue Saint-Leu,
80 000 Amiens, France.
e-mail : serge.dumont@u-picardie.fr

Abstract In this article, we present various numerical methods to solve multi-contact problems within the Non-Smooth Discrete Element Method. The techniques considered to solve the frictional unilateral conditions are based both on the bi-potential theory introduced by de Saxcé et al. [2] and the Augmented Lagrangian theory introduced by Alart et al. [1]. Following the ideas of Feng et al. [3], a new Newton method is developed to improve these classical algorithms and numerical experiments are presented to show that these methods are faster than the previous ones and provides results with a better quality.

Key words: Granular materials, Contact mechanics, Newton algorithms, Bi-potential, Augmented Lagrangian.

1 Introduction

This is a first draft of a paper that will be submitted in a near future.

The paper is organized as follow: in the next part, we present the equations to be solved for the Discrete Element Method, and the frictional contact law considered. In the third part, we first present two classical methods to numerically solve the full problem, the first one based on the bi-potential theory, and the second one on the Augmented Lagrangian theory. Then, we show how these methods can be enhanced using an appropriate Newton method. The last part on this article is devoted to the numerical experiments in order to show the main properties of these algorithms.

2 Problem Setting

2.1 The equations of motion of a multi-contact system

Classically (see for example [8, 7, 11]), the motion of a multi-contact system is described using a global generalized coordinate \mathbf{q} (for N_p particles, $\mathbf{q} \in \mathbb{R}^{\tilde{d} \times N_p}$, where $\tilde{d} = 6$ for a 3D problem and $\tilde{d} = 3$ for a 2D problem). Due to the possible shocks between particles, the equations of motion has to be formulated in term of differential measure equation:

$$\mathbb{M}d\dot{\mathbf{q}} + \mathbf{F}^{int}(t, \mathbf{q}, \dot{\mathbf{q}})dt = \mathbf{F}^{ext}(t, \mathbf{q}, \dot{\mathbf{q}})dt + d\mathbf{R} \quad (1)$$

where

- \mathbb{M} represents the generalized mass matrix;
- \mathbf{F}^{int} and \mathbf{F}^{ext} represent the internal and external forces respectively;
- $d\mathbf{R}$ is a non-negative real measure, representing the reaction forces and impulses between particles in contact.

For the sake of simplicity and without lost of generality, only the external forces are considered in the following. The internal forces are neglected because the general case can be easily derived through a linearizing procedure.

Then, for the numerics, the equation (1) is integrated on each time interval $[t_k, t_{k+1}]$, and approximated using a θ -method with $\theta \in]\frac{1}{2}, 1]$ for stability reason (see [14]).

Therefore, the classical approximation of equation (1) yields

$$\begin{cases} \mathbb{M}(\dot{\mathbf{q}}_{k+1} - \dot{\mathbf{q}}_k) = \Delta t(\theta \mathbf{F}_{k+1} + (1 - \theta) \mathbf{F}_k) + \mathbf{R}_{k+1} \\ \mathbf{q}_{k+1} = \mathbf{q}_k + \Delta t \theta \dot{\mathbf{q}}_{k+1} + \Delta t(1 - \theta) \dot{\mathbf{q}}_k \end{cases} \quad (2)$$

We will denote $\dot{\mathbf{q}}_k^{free} = \dot{\mathbf{q}}_k + \mathbb{M}^{-1} \Delta t(\theta \mathbf{F}_{k+1} + (1 - \theta) \mathbf{F}_k)$ the free velocity (velocity when the contact forces vanish). Then, the first equation in (2) becomes

$$\dot{\mathbf{q}}_{k+1} = \dot{\mathbf{q}}_k^{free} + \mathbb{M}^{-1} \mathbf{R}_{k+1}. \quad (3)$$

In order to write the contact law, for a contact c between two particles ($1 \leq c \leq N_c$, where N_c is the total number of contact), we define the local-global mapping

$$\begin{cases} \mathbf{u}^c = P^*(\mathbf{q}, c) \dot{\mathbf{q}} \\ \mathbf{R} = P(\mathbf{q}, c) \mathbf{r}^c \end{cases} \quad (4)$$

where \mathbf{u}^c is the local relative velocity between the two bodies in contact and \mathbf{r}^c is the local contact forces ($\mathbf{u}^c, \mathbf{r}^c \in \mathbb{R}^d$ where d is the dimension of the problem, and P^* is the transpose of matrix P). We also denote $\mathbb{P}(\mathbf{q})$ the total-global mapping, for \mathbf{u} and \mathbf{r} in $\mathbb{R}^{d \times N_c}$ (vectors composed of all relative velocity and contact forces respectively):

$$\begin{cases} \mathbf{u} = \mathbb{P}^*(\mathbf{q}) \dot{\mathbf{q}} \\ \mathbf{R} = \mathbb{P}(\mathbf{q}) \mathbf{r} \end{cases} \quad (5)$$

In the discretization, a prediction of \mathbf{q} is computed to estimate the mapping $\mathbb{P}(\mathbf{q})$ (see equations (18) and (19) in the following).

Using the equations (2) and (5), the discretization of the motion of a multi-contact system, with frictional contact between particles can be written:

$$\begin{cases} \tilde{\mathbf{u}}_{k+1} = \tilde{\mathbf{u}}_k^{free} + \mathbb{W}\mathbf{r}_{k+1} \\ law_c(\tilde{\mathbf{u}}_{k+1}^c, \mathbf{r}_{k+1}^c) = \text{.true.} \end{cases} \quad \forall c \in \{1, 2, \dots, N_c\} \quad (6)$$

where $\mathbb{W} = \mathbb{P}^*\mathbb{M}^{-1}\mathbb{P}$ is the Delassus operator, and $\tilde{\mathbf{u}}_k^{free} = \mathbb{P}^*\dot{\mathbf{q}}_k^{free}$ is the relative free velocity. Notice that a Newton impact law is also considered (see [11] and equation (20) in the following), that modify \mathbf{u}_k and \mathbf{u}_k^{free} by $\tilde{\mathbf{u}}_k$ and $\tilde{\mathbf{u}}_k^{free}$ respectively.

The second equation in (6) is the implicit frictional contact law that is in our case the classical Signorini condition and Coulomb's friction law.

2.2 The frictional contact law

In the local coordinates system defined by the local normal vector \mathbf{n} and the tangential vector $\mathbf{t} \perp \mathbf{n}$, any element \mathbf{u} and \mathbf{r} can be uniquely decomposed as $\mathbf{u} = u_n\mathbf{n} + \mathbf{u}_t$ and $\mathbf{r} = r_n\mathbf{n} + \mathbf{r}_t$ respectively. In these coordinates, the unilateral contact law can be stated using the Signorini's conditions (see figure 1 for a graphical representation):

$$u_n \geq 0, \quad r_n \geq 0, \quad u_n r_n = 0. \quad (7)$$

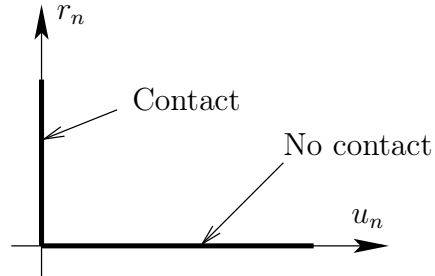


Figure 1: The Signorini conditions

On the other hand, the Coulomb's law of friction can be stated using the algorithmic

form (see figure 2 for a graphical representation):

$$\left[\begin{array}{lll} \text{If } r_n = 0 & \text{then } u_n \geq 0 & ! \text{ No contact} \\ \text{Else if } r_n > 0 \text{ and } \|\mathbf{r}_t\| < \mu r_n & \text{then } \mathbf{u} = 0 & ! \text{ Sticking} \\ \text{Else } r_n > 0 \text{ and } \|\mathbf{r}_t\| = \mu r_n & \text{then } \exists \lambda \geq 0 \text{ such that } \mathbf{u}_t = \lambda \frac{\mathbf{r}_t}{\|\mathbf{r}_t\|} & ! \text{ Sliding} \end{array} \right. \quad (8)$$

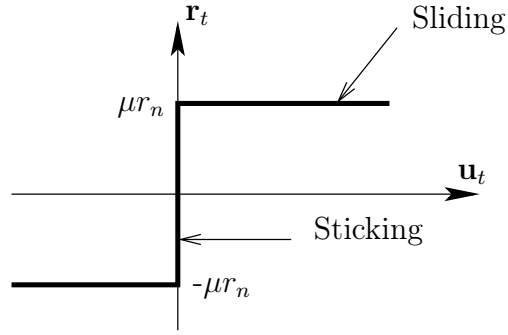


Figure 2: The Coulomb conditions

For a given friction coefficient μ , let K_μ be the isotropic Coulomb's cone, which defines the set of admissible forces (see figure 3):

$$K_\mu = \{\mathbf{r} = r_n \mathbf{n} + \mathbf{r}_t : \|\mathbf{r}_t\| - \mu r_n \leq 0\} \quad (9)$$

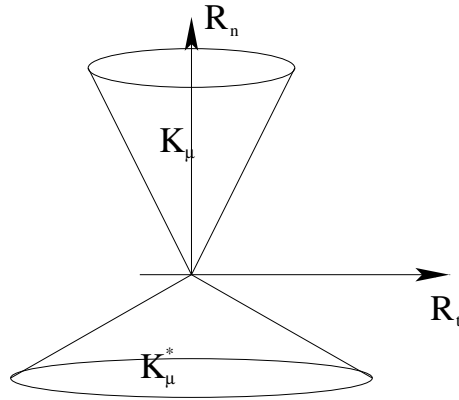


Figure 3: The Coulomb's cone

The previous law can be also written:

$$\left[\begin{array}{lll} \text{If } r_n = 0 & \text{then } u_n \geq 0 & ! \text{ No contact} \\ \text{Else if } \mathbf{r} \in I(K_\mu) & \text{then } \mathbf{u} = 0 & ! \text{ Sticking} \\ \text{Else } r_n > 0 \text{ and } \mathbf{r} \in B(K_\mu) & \text{then } \exists \lambda \geq 0 \text{ such that } \mathbf{u}_t = \lambda \frac{\mathbf{r}_t}{\|\mathbf{r}_t\|} & ! \text{ Sliding} \end{array} \right. \quad (10)$$

where $I(K_\mu)$ and $B(K_\mu)$ are respectively the interior and the boundary of the cone K_μ .

3 Numerical Resolution of the contact/friction problems

We will describe in this section the numerical algorithms that will be considered in the following. Generally, to solve the problem (6), the numerical algorithms considered are based on two levels: the global level where the equations of motion are solved, and the local level devoted to the resolution of the contact law.

3.1 Resolution of the global problem : the Non Linear Gauss Seidel Method (NLGS)

In this paragraph, we describe the algorithm used at the global level to solve the problem (6). Following the ideas of Jean and Moreau [8, 11], we use the non-linear Gauss-Seidel algorithm which is the most commonly used. It consists in considering successively each contact until the convergence. The numerical criterion used to state the convergence will be studied latter in the paper.

This method is intrinsically sequential but it is possible to used a simple multi-threading technique which consists in splitting the contact loop into several threads. This method has been studied in [16] in the case where the local algorithm is based on the Augmented Lagrangian method.

Notice that it is also possible to consider at this stage more sophisticated method such as a conjugate gradient type method (see for example [14]).

3.2 The standard bi-potential based method (SBP)

In this paragraph, we provide a first method to solve the contact problem, at the local level (contact point between two particles). The method is based on the notion of bi-potential, introduced by de Saxcé et al. [2].

Using the bi-potential framework, it can be shown (see for example [2, 4, 6, 21]) that a couple (\mathbf{u}, \mathbf{r}) verifies the Signorini-Coulomb contact rules if

$$b_c(\mathbf{v}, \mathbf{s}) + \mathbf{v} \cdot \mathbf{s} \geq b_c(\mathbf{u}, \mathbf{r}) + \mathbf{u} \cdot \mathbf{r} = 0 \quad \forall \mathbf{v}, \mathbf{s} \quad (11)$$

where b_c is the bi-potential

$$b_c(-\mathbf{u}, \mathbf{r}) = \Psi_{\mathbb{R}^+}(u_n) + \Psi_{K_\mu}(\mathbf{r}) + \mu r_n \|u_t\| \quad (12)$$

and Ψ_C stands for the indicatrix function of the set C : $\Psi_C(x) = 0$ if $x \in C$, $\Psi_C(x) = +\infty$ if $x \notin C$.

Consequently, the contact law can be written in a compact form of an implicit subnormality rule (or a differential inclusion rule):

$$-\mathbf{u} \in \partial_{\mathbf{r}} b_c(-\mathbf{u}, \mathbf{r}). \quad (13)$$

Then, for a contact c , at a NLGS iteration i , knowing the relative velocity $\tilde{\mathbf{u}}^{c,i}$, the algorithm to compute $\mathbf{r}^{c,i+1}$ from $\mathbf{r}^{c,i}$ is based on the minimization of the bi-potential (see for exemple [4], page 51), using the inequality:

$$b_c(-\tilde{\mathbf{u}}^{c,i}, \mathbf{r}) + \tilde{\mathbf{u}}^{c,i} \cdot \mathbf{r} \geq b_c(-\tilde{\mathbf{u}}^{c,i}, \mathbf{r}^{c,i+1}) + \tilde{\mathbf{u}}^{c,i} \cdot \mathbf{r}^{c,i+1} \quad \forall \mathbf{r} \in K_\mu \quad (14)$$

or $g(\mathbf{r}) \geq g(\mathbf{r}^{c,i+1})$, $\forall \mathbf{r} \in K_\mu$, if we denote

$$g(\mathbf{r}) = \Psi_{\mathbb{R}^+}(\tilde{u}_n^{c,i}) + \Psi_{K_\mu}(\mathbf{r}) + \mu r_n \|\tilde{\mathbf{u}}_t^{c,i}\| + \tilde{\mathbf{u}}^{c,i} \cdot \mathbf{r}. \quad (15)$$

The minimization of (14) is classically realized using a projected gradient projection (Uzawa method) without considering the singular term $\Psi_{\mathbb{R}^+}(\tilde{u}_n^{c,i})$. This minimization can also be viewed as the proximal point of the augmented force $\mathbf{r} - \rho \tilde{\mathbf{u}}$, with respect to the function $\mathbf{r} \mapsto \rho b_c(-\tilde{\mathbf{u}}, \mathbf{r})$ (see for example [2, 4, 6]):

$$\mathbf{r} = \text{prox}(\mathbf{r} - \rho \tilde{\mathbf{u}}, \rho b_c(-\tilde{\mathbf{u}}, \mathbf{r})).$$

More precisely, the Uzawa method leads to compute the augmented force $\tau^{c,i+1} = \mathbf{r}^{c,i} - \rho \nabla \tilde{g}(\mathbf{r}^{c,i})$, where \tilde{g} is the differential part of g :

$$\nabla \tilde{g}(\mathbf{r}^{c,i}) = \nabla_{\mathbf{r}}(\mu r_n \|\tilde{\mathbf{u}}_t^{c,i}\| + \tilde{\mathbf{u}}^{c,i} \cdot \mathbf{r}) = \mu \|\tilde{\mathbf{u}}_t^{c,i}\| \mathbf{n} + \tilde{\mathbf{u}}^{c,i},$$

and to consider the force at next step as a projection of the augmented force onto the set of admissible force $\mathbf{r}^{c,i+1} = \text{proj}(\tau^{c,i+1}, K_\mu)$, that provides equations (21) and (22) in the resolution algorithm of the global problem. The $\text{proj}(\tau^{c,i+1}, K_\mu)$ stands for the orthogonal projection over the convex K_μ , that can be computed exactly (see [4]).

This algorithm will be referred as the SBP (Standard Bi-Potential) method above and throughout.

For a sake of simplicity, we denote hereafter the descent direction

$$\mathbf{D}^{c,i} = \mu \|\tilde{\mathbf{u}}_t^{c,i}\| \mathbf{n} + \tilde{\mathbf{u}}^{c,i}.$$

Remark 1 *A first improvement of this method could be to compute the optimal step $\rho^{c,i}$. To do so, we have to minimize*

$$\rho \mapsto g(\mathbf{r}^{c,i} - \rho \mathbf{D}^{c,i}), \quad (16)$$

or, more precisely,

$$\begin{aligned} \rho \mapsto & \Psi_{\mathbb{R}^+}(\tilde{u}_n^{c,i}) + \Psi_{K_\mu}(\mathbf{r}^{c,i} - \rho \mathbf{D}^{c,i}) + \mu(r_n^{c,i} - \rho \mathbf{D}^{c,i} \cdot \mathbf{n}) \|\tilde{\mathbf{u}}_t^{c,i}\| + \tilde{\mathbf{u}}_t^{c,i} \cdot (\mathbf{r}^{c,i} - \rho \mathbf{D}^{c,i}) \\ & = \Psi_{\mathbb{R}^+}(\tilde{u}_n^{c,i}) + \Psi_{K_\mu}(\mathbf{r}^{c,i} - \rho \mathbf{D}^{c,i}) - \rho \mathbf{D}^{c,i} \cdot (\mu \|\tilde{\mathbf{u}}_t^{c,i}\| \mathbf{n} + \tilde{\mathbf{u}}_t^{c,i}) + Cte \\ & = \Psi_{\mathbb{R}^+}(\tilde{u}_n^{c,i}) + \Psi_{K_\mu}(\mathbf{r}^{c,i} - \rho \mathbf{D}^{c,i}) - \rho \|\mathbf{D}^{c,i}\|^2 + Cte. \end{aligned} \quad (17)$$

We can observe that this method do not permit to choose an optimal parameter ρ since g , as a function of ρ , is linear, excepted in the case where $\mathbf{D}^{c,i} \notin K_\mu$. A solution could be to modify the function g , for example by replacing $\tilde{\mathbf{u}}^{c,i}$ by a prediction of $\tilde{\mathbf{u}}^{c,i+1}$ using the equations of the dynamics. Unfortunately, this method do not provides good numerical results.

Then, the standard bi-potential based algorithm (SBP) can be written (see [21] for example):

- Loop on the step time k
 - Prediction of a position (for the computation of the local-global mapping):

$$\mathbf{q}_{k+\frac{1}{2}} = \mathbf{q}_k + \frac{\Delta t}{2} \dot{\mathbf{q}}_k; \quad (18)$$

- Initialization of the motion: $\dot{\mathbf{q}}_{k+1}^0 = \dot{\mathbf{q}}_k^{free}$ (initialization of the contact forces with $\mathbf{R} = 0$).
- Loop on $i \geq 0$ (NLGS), until convergence

* Loop on the contacts c :

- Computation of the local-global mapping

$$\dot{\mathbf{u}}^- = P^*(\mathbf{q}_{k+\frac{1}{2}}, c) \dot{\mathbf{q}}_k; \quad \dot{\mathbf{u}}^{c,+i} = P^t(\mathbf{q}_{k+\frac{1}{2}}, c) \dot{\mathbf{q}}_{k+1}^i \quad (19)$$

- Newton shock law

$$\tilde{u}_n^{c,i} = \frac{u_n^{c,+i} + e_n u_n^-}{1 + e_n}; \quad \tilde{\mathbf{u}}_t^{c,i} = \frac{\mathbf{u}_t^{c,+i} + e_n \mathbf{u}_t^-}{1 + e_t} \quad (20)$$

- Prediction of the reaction:

$$\tau^{c,i+1} = \mathbf{r}^{c,i} - \rho \left[\tilde{\mathbf{u}}_t^{c,i} + (\tilde{u}_n^{c,i} + \mu \|\tilde{\mathbf{u}}_t^{c,i}\|) \mathbf{n} \right] \quad (21)$$

- Correction of the reaction:

$$\mathbf{r}^{c,i+1} = \text{proj}(\tau^{c,i+1}, K_\mu) \quad (22)$$

- Actualization of the generalized displacement:

$$\dot{\mathbf{q}}_{k+1}^{i+1} = \dot{\mathbf{q}}_k^{free} + \mathbb{M}^{-1} \left(\sum_{\alpha \leq c} P(\mathbf{q}_{k+\frac{1}{2}}, \alpha) \mathbf{r}^{\alpha,i+1} + \sum_{\alpha > c} P(\mathbf{q}_{k+\frac{1}{2}}, \alpha) \mathbf{r}^{\alpha,i} \right) \quad (23)$$

- * End of the loop on contacts c .

- End of the loop on i of NLGS when the convergence is reached: $\dot{\mathbf{q}}_{k+1} = \dot{\mathbf{q}}_{k+1}^{i+1}$
- Actualization of the generalized displacements: $\mathbf{q}_{k+1} = \mathbf{q}_{k+\frac{1}{2}} + \frac{\Delta t}{2} \dot{\mathbf{q}}_{k+1}$

- End of the loop on the step time k .

Remark 2 Notice that only one iteration of the Uzawa algorithm at the local level is considered. Various previous studies (see for example [9]) show that there is no significant improvement of the method if several iterations of the Uzawa algorithm are considered at this stage.

3.3 Newton method and enhanced bi-potential method (EBP)

We introduce in this section a Newton method in order to speed up the convergence of the computation of the solution. This method has been already used, especially in the case of the augmented lagrangian method developed by Alart et al. [1], and the ideas presented in this article follows those of Feng et al. [3] and have been adapted to the problem of the discrete element method. The main idea of this technique is to find the solution of the optimization problem, not as a minimum of a functional, but rather as a zero of a function, using the Euler equation of the problem. Then a standard Newton method can be developed to solve this Euler equation.

The technique is first described in the case of the bi-potential framework, and will be adapted to the augmented lagrangian method farther.

We recall that the local problem that has to be solved, for each contact c can be written

$$\begin{cases} \tilde{\mathbf{u}}_{k+1}^c = \tilde{\mathbf{u}}_k^{c,free} + \sum_{\alpha=1}^{N_c} W_{c\alpha} \mathbf{r}^\alpha \\ \mathbf{r}^c = \text{proj}(\tau^c, K_\mu) \end{cases} \quad \forall c = 1, \dots, N_c \quad (24)$$

where $\tau^c = \mathbf{r}^c - \rho(\mu \|\tilde{\mathbf{u}}_t^c\| \mathbf{n} + \tilde{\mathbf{u}})$ is the augmented reaction (see 21), and $W_{c\alpha} = P^*(\mathbf{q}_{k+\frac{1}{2},c}) \mathbb{M}^{-1} P(\mathbf{q}_{k+\frac{1}{2},\alpha})$ is the local Delassus operator.

This problem can be written equivalently

$$\begin{cases} \tilde{\mathbf{u}}_{k+1}^c - \tilde{\mathbf{u}}_k^{c,free} - \sum_{\alpha=1}^{N_c} W_{c\alpha} \mathbf{r}^\alpha = 0 \\ \mathbf{r}^c - \text{proj}(\tau^c, K_\mu) = 0 \end{cases} \quad \forall c = 1, \dots, N_c \quad (25)$$

Reminding now that we want to use a Newton algorithm to solve these equations inside the Non Linear Gauss Seidel loop on the variable i , we define now, for each contact $c = 1, \dots, N_c$, the function

$$f_c^i(\chi) = \begin{pmatrix} \tilde{\mathbf{u}}^{c,i} - \tilde{\mathbf{u}}_k^{c,free} - \sum_{\alpha=1}^{N_c} W_{c\alpha} \mathbf{r}^{\alpha,i} \\ \mathbf{Z}^{c,i} \end{pmatrix}$$

where :

- the vector \mathbf{Z}^c is the error on the prediction of the reaction

$$\mathbf{Z}^{c,i}(\mathbf{r}^{c,i}, \tilde{\mathbf{u}}^{c,i}) = \mathbf{r}^{c,i} - \text{proj}(\tau^{c,i}, K_\mu), \quad (26)$$

- $\chi_c = (\mathbf{r}^{c,i}, \tilde{\mathbf{u}}^{c,i})^t$,
- $\chi = (\chi_1, \chi_2, \dots, \chi_{N_c})^t$

Remark 3 *The first equality in the relation $f(\chi) = 0$ is the equation of motion for the bodies in contact, and the second relation is the frictional Coulomb law between the bodies in contact, written within the bipotential framework.*

Then we have to write a Newton algorithm to solve the problem $f(\chi) = 0$. This algorithm can be written, for a contact c , by substituting equations (21) and (22) in algorithm (SBP) by the followings:

- Initialization:

$$\chi_c^0 = (\mathbf{r}^0 = \mathbf{r}^{c,i}, \mathbf{v}^0 = \tilde{\mathbf{u}}^{c,i})^t, \quad \ell = 0$$

- Loop on ℓ , until convergence:

$$- \tau_\ell^c = \mathbf{r}^\ell - \rho(\mu \|\mathbf{v}_t^\ell\| \mathbf{n} + \mathbf{v}^\ell)$$

- Resolution:

$$\left[\frac{\partial f_c}{\partial \chi^c}(\chi^\ell) \right] \Delta \chi_c = -f_c(\chi^\ell) \quad (27)$$

- Actualization: $\chi_c^{\ell+1} = \chi_c^\ell + \Delta\chi_c$
- End of the loop on ℓ until convergence, $\tilde{\mathbf{u}}^{c,i+1} = \mathbf{v}^\ell$ and $\mathbf{r}^{c,i+1} = \mathbf{r}^\ell$.

Remark 4 *This algorithm needs more than one iteration at each Non Linear Gauss Seidel iteration to be efficient. As a consequence and compared to the Uzawa algorithm, the solution in the Newton algorithm is controlled by both the local (iteration ℓ) and global convergence criteria (iteration i , see [3, 9]).*

The local convergence criterion for the Newton algorithm is defined by:

$$\varepsilon_{Newt}^c(\chi_\ell) = \|\mathbf{v}^\ell - \mathbf{u}_k^{c,free} - W\mathbf{r}^\ell\| + \|\mathbf{r}^\ell - \text{proj}(\mathbf{r}^\ell, K_\mu)\| \quad (28)$$

This criterion measure $f_c(\chi_\ell)$ that has to be sufficiently small.

The matrix $\left[\frac{\partial f_c}{\partial \chi_c}(\chi)\right]$ represents the tangential matrix of the local equations for the contact c . This matrix is of dimension 6×6 for a 3 dimensional problem, and 3×3 for a 2 dimensional problem. For a 3 dimensional problem, the general form of this matrix is the following:

$$\left[\frac{\partial f_c}{\partial \chi_c}(\chi)\right] = \begin{bmatrix} -W & Id_{3 \times 3} \\ A_c & B_c \end{bmatrix} \quad (29)$$

where

$$A_c = \left[\frac{\partial Z_c}{\partial r_n} \mid \frac{\partial Z_c}{\partial r_{t_1}} \mid \frac{\partial Z_c}{\partial r_{t_2}}\right] \quad B_c = \left[\frac{\partial Z_c}{\partial v_n} \mid \frac{\partial Z_c}{\partial v_{t_1}} \mid \frac{\partial Z_c}{\partial v_{t_2}}\right] \quad (30)$$

The matrices A_c and B_c takes different forms according to the contact status:

- First case: sliding contact.

In that case, we have

$$\mu\|\tau_t\| \geq -\tau_n \quad \|\tau_t\| \geq \mu\tau_n$$

then

$$\text{Proj}(\tau, K_\mu) = \tau - \left(\frac{\|\tau_t\| - \mu\tau_n}{1 + \mu^2}\right) \left(\frac{\tau_t}{\|\tau_t\|} - \mu\mathbf{n}\right)$$

and

$$\mathbf{Z}_c = \rho(\mu\|\mathbf{v}_t^k\|\mathbf{n} + \mathbf{v}^k) + \left(\frac{\|\tau_t\| - \mu\tau_n}{1 + \mu^2}\right) \left(\frac{\tau_t}{\|\tau_t\|} - \mu\mathbf{n}\right)$$

The computation of the derivatives of \mathbf{Z}_c provides the matrices A_c and B_c :

$$\begin{aligned} -\frac{\partial \mathbf{Z}_c}{\partial r_n} &= -\frac{\mu}{1 + \mu^2} \left(\frac{\tau_t}{\|\tau_t\|} - \mu\mathbf{n}\right) \\ -\frac{\partial \mathbf{Z}_c}{\partial r_{t_1}} &= \frac{\tau_{t_1}}{(1 + \mu^2)\|\tau_t\|} \left(\frac{\tau_t}{\|\tau_t\|} - \mu\mathbf{n}\right) + \frac{\|\tau_t\| - \mu\tau_n}{1 + \mu^2} \left(\frac{\mathbf{t}_1}{\|\tau_t\|} - \frac{\tau_{t_1}}{\|\tau_t\|^3}\tau_t\right) \end{aligned}$$

$$\begin{aligned}
-\frac{\partial \mathbf{Z}_c}{\partial r_{t_2}} &= \frac{\tau_{t_2}}{(1+\mu^2)\|\tau_t\|} \left(\frac{\tau_t}{\|\tau_t\|} - \mu \mathbf{n} \right) + \frac{\|\tau_t\| - \mu \tau_n}{1+\mu^2} \left(\frac{\mathbf{t}_2}{\|\tau_t\|} - \frac{\tau_{t_2}}{\|\tau_t\|^3} \tau_t \right) \\
-\frac{\partial \mathbf{Z}_c}{\partial v_n} &= \rho \mathbf{n} + \frac{\rho \mu}{1+\mu^2} \left(\frac{\tau_t}{\|\tau_t\|} - \mu \mathbf{n} \right) \\
-\frac{\partial \mathbf{Z}_c}{\partial v_{t_1}} &= \rho \left(\mathbf{t}_1 + \mu \frac{v_{t_1}}{\|\mathbf{v}_t\|} \mathbf{n} \right) - \frac{\rho}{1+\mu^2} \left(\left(\frac{\tau_{t_1}}{\|\tau_t\|} - \frac{\mu^2 v_{t_1}}{\|\mathbf{v}_t\|} \right) \left(\frac{\tau_t}{\|\tau_t\|} - \mu \mathbf{n} \right) + \right. \\
&\quad \left. (\|\tau_t\| - \mu \tau_n) \left(\frac{\mathbf{t}_1}{\|\tau_t\|} - \frac{\tau_{t_1}}{\|\tau_t\|^3} \tau_t \right) \right) \\
-\frac{\partial \mathbf{Z}_c}{\partial v_{t_2}} &= \rho \left(\mathbf{t}_2 + \mu \frac{v_{t_2}}{\|\mathbf{v}_t\|} \mathbf{n} \right) - \frac{\rho}{1+\mu^2} \left(\left(\frac{\tau_{t_2}}{\|\tau_t\|} - \frac{\mu^2 v_{t_2}}{\|\mathbf{v}_t\|} \right) \left(\frac{\tau_t}{\|\tau_t\|} - \mu \mathbf{n} \right) + \right. \\
&\quad \left. (\|\tau_t\| - \mu \tau_n) \left(\frac{\mathbf{t}_2}{\|\tau_t\|} - \frac{\tau_{t_2}}{\|\tau_t\|^3} \tau_t \right) \right)
\end{aligned}$$

For a 2D problem, these computations yields:

$$\begin{aligned}
-\frac{\partial \mathbf{Z}_c}{\partial r_n} &= \frac{\mu}{1+\mu^2} (\mu \mathbf{n} - \theta_r \mathbf{t}) \\
-\frac{\partial \mathbf{Z}_c}{\partial r_t} &= \frac{1}{(1+\mu^2)} (-\mu \theta_r \mathbf{n} + \mathbf{t}) \\
-\frac{\partial \mathbf{Z}_c}{\partial v_n} &= \frac{\rho}{1+\mu^2} (\mathbf{n} + \mu \theta_r \mathbf{t}) \\
-\frac{\partial \mathbf{Z}_c}{\partial v_t} &= \frac{\rho \mu}{1+\mu^2} ((\theta_v + \theta_r) \mathbf{n} + \mu(1 - \theta_r \theta_v) \mathbf{t})
\end{aligned}$$

where $\theta_v = \text{sign}(\mathbf{v}_t)$ and $\theta_r = \text{sign}(\tau_t)$.

- Second case: sticking contact.

In that case, we have

$$\mu \|\tau_t\| \geq -\tau_n \quad \|\tau_t\| < \mu \tau_n$$

then

$$\mathbf{Z}_c = \rho(\mu \|\mathbf{v}_t^k\| \mathbf{n} + \mathbf{v}^k)$$

and the computation of the derivatives of \mathbf{Z}_c reads:

$$\begin{aligned}
-A_c &= 0_{3 \times 3} \\
-\frac{\partial \mathbf{Z}_c}{\partial v_n} &= \rho \mathbf{n} \\
-\frac{\partial \mathbf{Z}_c}{\partial v_{t_1}} &= \rho \mu \frac{v_{t_1}}{\|\mathbf{v}_t\|} \mathbf{n} + \rho \mathbf{t}_1 \\
-\frac{\partial \mathbf{Z}_c}{\partial v_{t_2}} &= \rho \mu \frac{v_{t_2}}{\|\mathbf{v}_t\|} \mathbf{n} + \rho \mathbf{t}_2
\end{aligned}$$

For a 2D problem, these computations leads to:

$$\begin{aligned} - A_c &= 0_{2 \times 2} \\ - \frac{\partial \mathbf{Z}_c}{\partial v_n} &= \rho \mathbf{n} \\ - \frac{\partial \mathbf{Z}_c}{\partial v_t} &= \rho \mu \theta_v \mathbf{n} + \rho \mathbf{t} \end{aligned}$$

- Third case: no contact.

In that case, the matrices $A_c = \text{Id}_{3 \times 3}$ and B_c vanishes, and $\chi_c^{\ell+1} = \begin{Bmatrix} 0 \\ \mathbf{v}^k \end{Bmatrix}$

3.4 Resolution of the linear system

Generally, the drawback of a Newton is the computational cost of the linear system to be solved at each iteration. Here, the particular form of the tangent matrix allows the use of a condensation technique. More precisely, the linear system to be solved can be written:

$$\begin{bmatrix} -W & \text{Id}_{3 \times 3} \\ A_c & B_c \end{bmatrix} \begin{pmatrix} \delta \mathbf{r} \\ \delta \mathbf{v} \end{pmatrix} = \begin{pmatrix} -\mathbf{f} \\ -\mathbf{g} \end{pmatrix}. \quad (31)$$

The first equation yields $\delta \mathbf{v} = -\mathbf{f} + W\delta \mathbf{r}$, and introducing this equality in the second equation leads to solve the linear system

$$(A_c + B_c W)\delta \mathbf{r} = -\mathbf{g} + B_c \mathbf{f}. \quad (32)$$

This properties halves the size of the linear system to be solved.

Remark 5 *A drawback of the bi-potential framework is that, due to its specificity, it is rather difficult to consider fully coupled problems, where the contact law and another phenomena, such as electricity or thermic effects are strongly coupled. The other method presented in this paper has a better property from this point of view because it is based on a more standard mathematical background in the theory of optimization.*

3.5 Newton method and enhanced augmented lagrangian method, (SAL) and (EAL)

In [1], Alart et al. propose another method to solve the frictional contact problem. This method has been also used with various improvement (parallelization, conjugate gradient method for example) to solve multi-contact problems [14, 15, 16, 17, 18]. Even if the coupled frictional contact problem is not an optimization problem anymore, it is always possible to formally formulate a “quasi”- optimization problem, for which the constraint

set depends on the normal components of the solution as a parameter. The solution is then searched as a saddle point of a "quasi" augmented Lagrangian of the problem.

More precisely, the global problem on all unknowns that has to be solved at each time step (in place of equation (24)) has the following form:

$$\begin{cases} \mathbf{u} = \mathbf{u}^{free} + \mathbb{W}\mathbf{r} \\ \mathbf{r} \geq 0, \mathbf{u} \geq 0, \mathbf{r} \cdot \mathbf{u} = 0. \end{cases} \quad (33)$$

In order to solve this problem, for a given $\mathbf{r} \in \mathbb{R}^{3 \times N_c}$, one can define the cartesian product of infinite half cylinder with section equal to the ball $\mathcal{B}(0, \mu r_c)$ of radius μr_c by:

$$\mathcal{C}(\mu\mathbf{r}) = \prod_{c=1}^{N_c} \mathbb{R}^+ \times \mathcal{B}(0, \mu r_c)$$

and then, the granular type frictional contact problem is given by

$$\mathbf{r} \in \operatorname{argmin}_{\mathbf{r} \in \mathcal{C}(\mu\mathbf{r})} \frac{1}{2} \mathbf{r} \cdot \mathbb{W}\mathbf{r} + \mathbf{u}^{free} \cdot \mathbf{r} = \operatorname{argmin}_{\mathbf{r} \in \mathcal{C}(\mu\mathbf{r})} J(\mathbf{r}), \quad (34)$$

and the projected gradient method the minimize this problem reads (for each iteration i of the NLGS algorithm):

$$\mathbf{r}^{i+1} = \operatorname{proj}(\mathbf{r}^i - \rho(\mathbf{u}^{free} + \mathbb{W}\mathbf{r}^i), \mathcal{C}(\mu\mathbf{r}^{i+1})), \quad (35)$$

or $\mathbf{r}^{i+1} = \operatorname{proj}(\tau^{i+1}, \mathcal{C}(\mu\mathbf{r}^{i+1}))$, with $\tau^{i+1} = \mathbf{r}^i - \rho\mathbf{u}^i$, $\mathbf{u}^i = \mathbf{u}^{free} + \mathbb{W}\mathbf{r}^i$. This algorithm will be referred to hereinafter as the SAL (Simple Augmented Lagrangian) method.

Notice that this method is very closed to the SBP method. More precisely, for a contact c , only the descent direction $\tilde{\mathbf{u}}^{c,i} + \mu\|\tilde{\mathbf{u}}_t^{c,i}\|\mathbf{n}$ in (21) is replaced by $\tilde{\mathbf{u}}^{c,i}$ and the projection $\mathbf{r}^{c,i+1} = \operatorname{proj}(\tau^{c,i+1}, K_\mu)$ in (23) is replaced by

$$\begin{cases} r_n^{c,i+1} = \max(0, \tau_n^{c,i+1}) \\ \mathbf{r}_t^{c,i+1} = \frac{\tau_t^{c,i+1}}{\|\tau_t^{c,i+1}\|} \mu r_n^{c,i+1}. \end{cases}$$

Remark 6 *On the contrary, it is possible to see the algorithm developed from the bi-potential formalism as a slight modification of the algorithm above. Indeed, it is only*

necessary to change the set $\mathcal{C}(\mathbf{r})$ by $\mathcal{K} = \prod_{c=1}^{N_c} K_\mu$, and to change the descent direction $\tilde{\mathbf{u}}^{c,i}$ by $\tilde{\mathbf{u}}^{c,i} + \mu\|\tilde{\mathbf{u}}_t^{c,i}\|\mathbf{n}$ which remains a descent direction for the SAL method, since

$$\nabla J(\mathbf{r}^{c,i+1}) \cdot \mathbf{D}^{c,i} = -\|\tilde{\mathbf{u}}^{c,i}\|^2 - \tilde{\mathbf{u}}^{c,i} \cdot (\mu\|\tilde{\mathbf{u}}_t^{c,i}\|\mathbf{n}) = -\|\tilde{\mathbf{u}}^{c,i}\|^2 - \mu u_n^{c,i} \|\tilde{\mathbf{u}}_t^{c,i}\|$$

which is negative since $\mu \in [0, 1]$.

Then, acting by analogy, we can develop a Newton method to find the minimum of J by seeking the solution as a zero of the function $\tilde{f}(\chi)$ where, for a contact c

$$\tilde{f}_c(\chi) = \begin{pmatrix} \tilde{\mathbf{u}}_{k+1}^c - \tilde{\mathbf{u}}_k^{c,free} - \sum_{\alpha=1}^{N_c} W_{c\alpha} \mathbf{r}^\alpha \\ \tilde{\mathbf{Z}}^c \end{pmatrix},$$

the vector $\tilde{\mathbf{Z}}^c$ is the error on the prediction of the reaction

$$\tilde{\mathbf{Z}}^c(\mathbf{r}^c, \tilde{\mathbf{u}}_{k+1}^c) = \mathbf{r}^c - \text{proj}(\tau_{k+1}^c, \mathcal{C}_c(\mu\tau_{k+1}^c)), \quad (36)$$

and the set $\mathcal{C}_c(\mu\mathbf{r}^c)$ is the set of admissible forces $\mathcal{C}_c(\mu\mathbf{r}^c) = \mathbb{R}^+ \times \mathcal{B}(0, r_c)$. This method will be referred as the EAL (Enhanced Augmented Lagrangian) method hereafter.

Then, as bellow, we have three cases in the computation of the tangent matrix $\left[\frac{\partial \tilde{f}}{\partial \chi^c}(\chi^\ell) \right]$:

- First case: sliding contact ($\tau_n > 0, \tau_t \geq \mu\tau_n$)

We have: $\text{proj}(\tau^c, \mathcal{C}_c(\mu\tau^c)) = \tau_n \mathbf{n} + \frac{\tau_t}{\|\tau_t\|} \mu\tau_n \mathbf{t}$ and $\tilde{\mathbf{Z}}_c = \rho v_n \mathbf{n} - \frac{\tau_t}{\|\tau_t\|} \mu\tau_n + \mathbf{r}_t$.

The computation of the derivatives of $\tilde{\mathbf{Z}}_c$ provides the matrices A_c and B_c :

$$\begin{aligned} -\frac{\partial \tilde{\mathbf{Z}}_c}{\partial r_n} &= -\mu \frac{\tau_t}{\|\tau_t\|} \\ -\frac{\partial \tilde{\mathbf{Z}}_c}{\partial r_{t_1}} &= \mathbf{t}_1 - \mu\tau_n \left(\frac{\mathbf{t}_1}{\|\tau_t\|} - \frac{\tau_{t_1}}{\|\tau_t\|^3} \tau_t \right) \\ -\frac{\partial \tilde{\mathbf{Z}}_c}{\partial r_{t_2}} &= \mathbf{t}_2 - \mu\tau_n \left(\frac{\mathbf{t}_2}{\|\tau_t\|} - \frac{\tau_{t_2}}{\|\tau_t\|^3} \tau_t \right) \\ -\frac{\partial \tilde{\mathbf{Z}}_c}{\partial v_n} &= \rho \left(\mathbf{n} + \mu \frac{\tau_t}{\|\tau_t\|} \right) \\ -\frac{\partial \tilde{\mathbf{Z}}_c}{\partial v_{t_1}} &= -\rho\mu\tau_n \left(\frac{\mathbf{t}_1}{\|\tau_t\|} - \frac{\tau_{t_1}}{\|\tau_t\|^3} \tau_t \right) \\ -\frac{\partial \tilde{\mathbf{Z}}_c}{\partial v_{t_2}} &= -\rho\mu\tau_n \left(\frac{\mathbf{t}_2}{\|\tau_t\|} - \frac{\tau_{t_2}}{\|\tau_t\|^3} \tau_t \right) \end{aligned}$$

For a two dimensional problem, these computations yields

$$A_c = \begin{pmatrix} 0 & 0 \\ -\mu\theta_r & 1 \end{pmatrix} \quad B_c = \begin{pmatrix} 1 & 0 \\ \mu\theta_r & 0 \end{pmatrix}.$$

- Second case: sticking contact ($\tau_n > 0, \tau_t < \mu\tau_n$)

$\text{proj}(\tau^c, \mathcal{C}_c(\mu\tau^c)) = \tau^c$ and the computation of the derivatives of \mathbf{Z}_c reads

- $A_c = 0_{3 \times 3}$
- $B_c = \rho \text{Id}_{3 \times 3}$

- Third case: no contact ($\tau_n \leq 0$)

$\text{proj}(\tau^c, \mathcal{C}_c(\mu\tau^c)) = 0$, then the matrices $A_c = \text{Id}_{3 \times 3}$ and B_c vanishes, and $\chi_c^{\ell+1} = \begin{Bmatrix} 0 \\ \mathbf{v}^k \end{Bmatrix}$

3.6 The global stopping (convergence) criterion

We present in this paragraph the convergence criterion on the global non linear Gauss-Seidel iterations. This criterion, developed from that proposed in [5] has been extended in the case of the Newton and bi-potential (EBP) method, where some term are naturally vanishing in the original Uzawa and bi-potential (SBP) method. This criterion ε_{glob} has been written in such a way that if the solution verify that ε_{glob} is sufficiently small, then this solution has good properties on the equation of motion and Signorini Coulomb contact law. Consequently, this criterion stays valid for the methods developed with the augmented lagrangian (SAL and EAL methods).

This criterion can be stated:

$$\varepsilon_{glob} = \frac{1}{N_c} \sum_{c=1}^{N_c} [\varepsilon_{motion}^c + \varepsilon_{proj}^c + \varepsilon_{b_c} + \varepsilon_{pen}^c] \quad (37)$$

where:

- $\varepsilon_{motion}^c = \|\tilde{\mathbf{u}}^c - \tilde{\mathbf{u}}_m^c\|$ where $\tilde{\mathbf{u}}_m^c = \tilde{\mathbf{u}}^{c,i} + \sum_{\alpha=1}^{N_c} W_{c\alpha} \mathbf{r}^\alpha$, so ε_{motion} measures the error on the equation of motion (see equation (24), this term vanishes for the SBP and SAL method);
- $\varepsilon_{proj}^c = \sqrt{\|\mathbf{r}^c - \text{proj}(\mathbf{r}^c, K_\mu)\|^2}$ is the error for the projection on the Coulomb cone (vanishing for the SBP method);
- $\varepsilon_{b_c} = \left| \tilde{\mathbf{u}}^c \cdot \mathbf{r}^c + \mu r_n^c \|\tilde{\mathbf{u}}_t^c\| \right|$ is the absolute value of the bi-potential that has to vanish if and only if the couple $(\tilde{\mathbf{u}}^c, \mathbf{r}^c)$ verifies the Signorini Coulomb contact law (see formula 11);
- $\varepsilon_{pen}^c = -\min(0, \tilde{u}_n^c)$ is the value of the penetration.

Remark 7 *One can notice that is absolutely necessary to verify in the criterion that there is no penetration, because nothing in the presented algorithm ensures that is condition is verify at the end of the loop. Moreover, if this condition is not satisfied, the rest of bi-potential can be negative or equal to zero, even if the couple $(\tilde{\mathbf{u}}, \mathbf{r})$ is not a solution.*

4 Numerical results

We present in the section three numerical examples with an increasing complexity.

In these computations, the descent parameter ρ is taken in such a way that the result is optimal, in terms of time computing. Denoting $\bar{\rho} = \frac{m_i m_j}{m_i + m_j} \frac{1}{\Delta t}$, for the SBP and the SAL methods, we have chosen $\rho = 0.6\bar{\rho}$, whereas for the EBP and the EAL methods, it is better to take $\rho = \bar{\rho}$. We recall that it has been shown that, for the bi-potential method (see for example [3]) and the augmented lagrangian method (see for example [14]), the parameter ρ has to verify $\rho < 2\bar{\rho}$ in order to ensure the convergence. Generally, for these two methods, the convergence is very sensitive on this parameter. We will show in the last paragraph of this study that for the EBP method, the parameter ρ can be taken in a large range around the value $\bar{\rho}$ without changing dramatically the convergence of the method.

At each iteration of the NLGS algorithm, the Newton algorithm is stopped either if the convergence is obtained ($\varepsilon_{Newt}^c \leq 10^{-5}$), or if the number of iteration of the Newton algorithm reached 100 when there is no convergence.

4.1 Ball sliding on a plane

In this first example, we consider a ball placed on a table with an initial horizontal velocity equal to $1.5 \text{ m} \cdot \text{s}^{-1}$. The ray of the ball is equal to $5 \cdot 10^{-3} \text{ m}$, and the friction coefficient between wall and ball is equal to $\mu = 0.7$. The time step of discretization is equal to 10^{-4} s . In this experiment, the ball first slides on the table, and then the ball rolls without slipping. The global stopping criterion is equal to $\varepsilon_{glob} = 10^{-10}$.

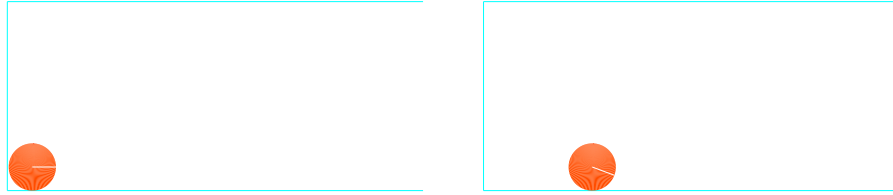


Figure 4: Example 1 – A ball is launched with an initial horizontal velocity (left). First, the ball slides. Then, the ball rolls without slipping (right).

Method	Number of NLGS iterations (last time step)	Error ε_{glob} (last time step)	Total CPU time (s)
SBP	18	$0.384 \cdot 10^{-10}$	9.44
SAL	18	$0.384 \cdot 10^{-10}$	9.28
EBP	1	0	8.83
EAL	1	$0.175 \cdot 10^{-13}$	8.78

Table 1: Comparison of the results obtained by the four methods on the first example (after the 2000th time step).

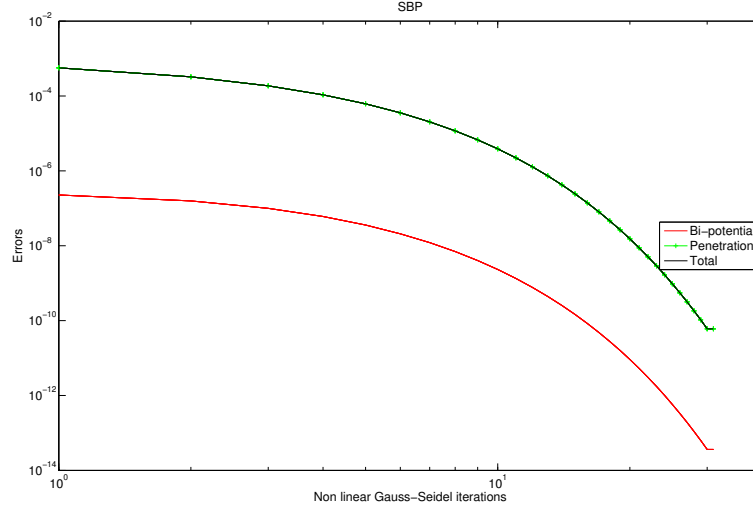


Figure 5: Example 1 – Convergence for the standard bi-potential based method, 5th iteration

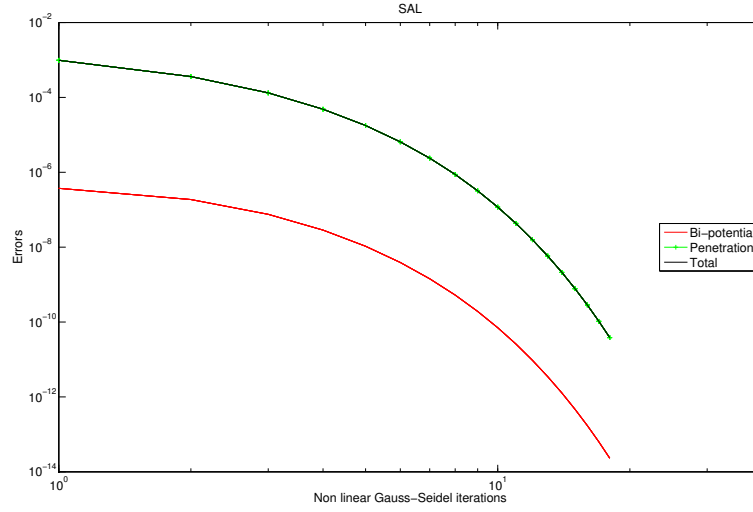


Figure 6: Example 1 – Convergence for the standard augmented lagrangian method, 5^{th} iteration

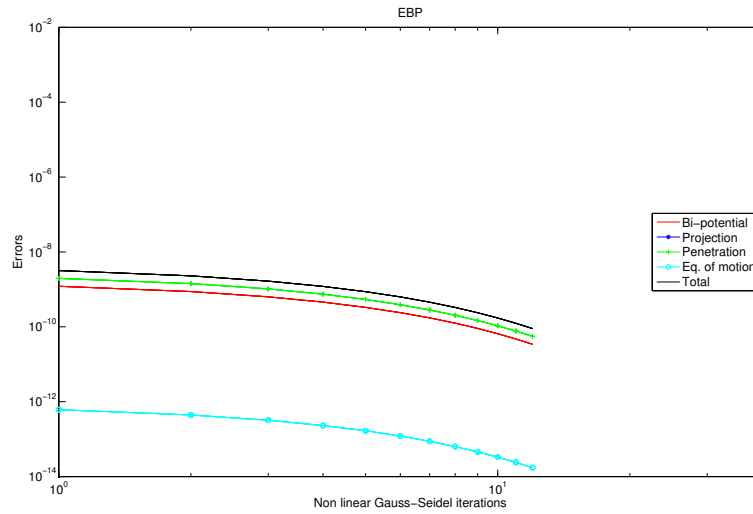


Figure 7: Example 1 – Convergence for the Newton and bi-potential method, 5^{th} iteration

We can observe from these numerical results that the error coming from the projection is very small for the four methods. The Standard Bi-Potential (SBP) method and the Standard Augmented Lagrangian method (SAL) give very closed results, both in term of quality (see figures 5 and 6) and in term of time computing (see table 1). Nevertheless, we can notice that the time computing is smaller with the SAL method, because there is less computations at each iteration (no term such as $\|\tilde{\mathbf{u}}_t\|$ and projection easier to compute for example). The Enhanced Bi-Potential method provides better results, both in term of quality (see figure 7) and in term of time computing (6.5% better). The Enhanced Augmented Lagrangian method converges after the first Non Linear Gauss Seidel iteration for every time steps, and consequently, this is the faster method on this example (7% faster than the SBP method).

4.2 Sedimentation of 4 balls in a box

In this second experiment, we consider the sedimentation of 4 balls of radius ranging from $4 \cdot 10^{-4}$ m to $5 \cdot 10^{-4}$ m. For the computations, the time step of discretization is equal to $\Delta t = 10^{-4}$ s., and the Non linear Gauss-Seidel loop is stopped either if the the global stopping criterion on the NLGS method is equal to $\varepsilon_{glob} = 10^{-10}$, or after 5000 iterations if there is no convergence (this case never occurs in this experiment). The friction coefficient between the balls and between the balls and the walls is equal to $\mu = 0.3$.

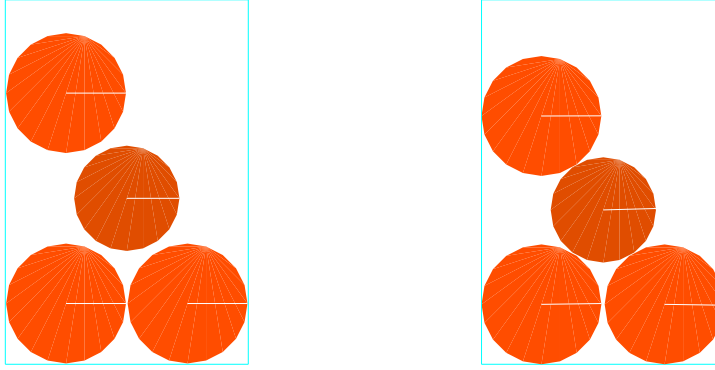


Figure 8: Example 2 – Sedimentation of four balls under the gravity effect.

Like in the previous simulation,, the SBP and the SAL method methods provide very similar results (see figures 9 and 10). For these two methods, we can notice that here the global error is essentially due to the penetrations. The SAL method is 2% faster than the SBP method (table 2).

Results obtained by the EBP method are better (figure 11), and here the overall error

Method	Number of NLGS iterations (last time step)	Error ε_{glob} (last time step)	Maximal penetration (last time step)	Total CPU time (s)
SBP	305	$0.949 \cdot 10^{-12}$	$0.310 \cdot 10^{-11}$	2.92
SAL	301	$0.980 \cdot 10^{-12}$	$0.340 \cdot 10^{-11}$	2.87
EBP	161	$0.635 \cdot 10^{-12}$	$0.641 \cdot 10^{-12}$	2.59
EAL	158	$0.973 \cdot 10^{-12}$	$0.208 \cdot 10^{-19}$	2.43

Table 2: Comparison of the results obtained by the four methods on the second example (after the 1000th time step)

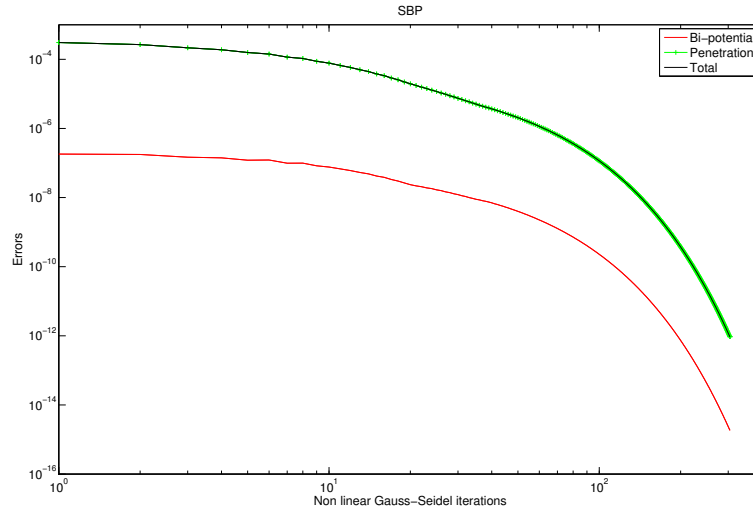


Figure 9: Example 2 – Convergence of the non-linear Gauss-Seidel iterations for the standard bi-potential based method (1000th time step) The two last curves overlaps, showing that the global error is governed by the error of penetration.

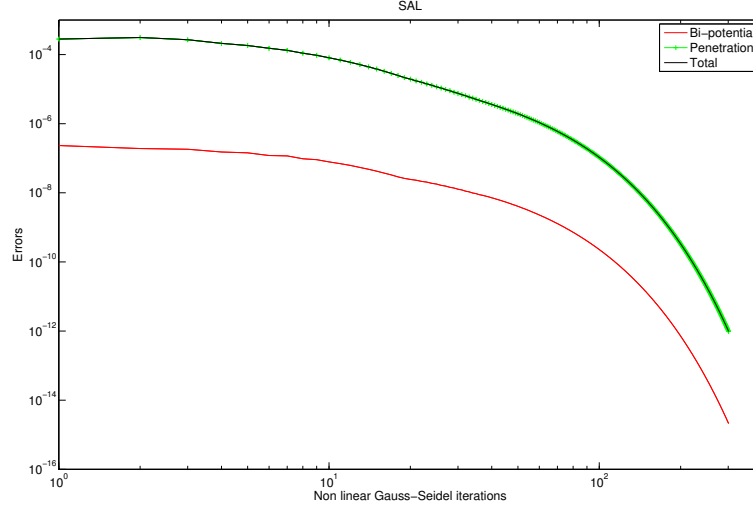


Figure 10: Example 2 – Convergence of the non-linear Gauss-Seidel iterations for the standard augmented lagrangian method (1000th time step). The two last curves overlaps, showing that the global error is governed by the error of penetration.

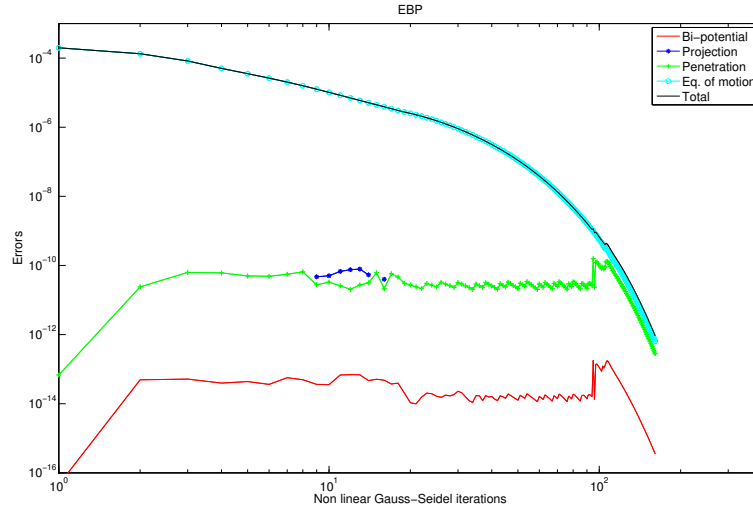


Figure 11: Example 2 – Convergence of the non-linear Gauss-Seidel iterations for the Newton and bi-potential method (1000th time step). The two last curves overlaps, that shows that the global error is governed by the error on the equations of motion.

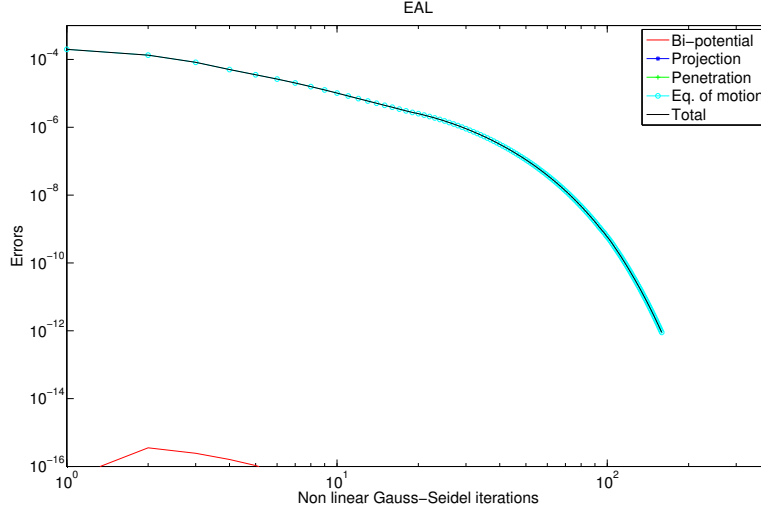


Figure 12: Example 2 – Convergence of the non-linear Gauss-Seidel iterations for the Newton and Augmented Lagrangian method (1000th time step). The two last curves overlaps, and the other ones does not appear on the figure because the corresponding errors are lower than 10^{-16} .

is governed by the error on the equations of the motion. The EBP method is 11% faster than the SBP method, and the penetration is 5 times smaller. In this example the EAL is the faster method (16,8% faster than the SBP method), and the penetration is very small (see figure 12).

4.3 Sedimentation of 500 balls

In this example, we consider the sedimentation of 500 balls (see figure 13) of radii ranging from $2.5 \cdot 10^{-4}$ m to $5 \cdot 10^{-4}$ m, the time step of discretization is equal to $\Delta t = 5 \cdot 10^{-5}$ s, and the Non linear Gauss-Seidel loop is stopped if the global estimator (37) verifies $\varepsilon_{glob} \leq 10^{-12}$ or after after 5000 iterations if there is no convergence. The friction coefficient between the balls and between the balls and the walls is equal to $\mu = 0.3$.

The results in table 3 are obtained after 1000 time steps.

In this example, the difference between methods SBP and SAL on the one hand, and the method EBP and EAL on the other hand is larger (see table 3). We can notice that the SAL method is 10.95% faster than the SBP method, and the EBP is 21.83% faster than the SBP method. Here, the EAL method is no longer the faster one, but the penetration is very small. Again, for the two first methods the global error is essentially due to the penetrations whereas the two last methods, the error is essentially due to the failure to follow precisely the equations of motion.

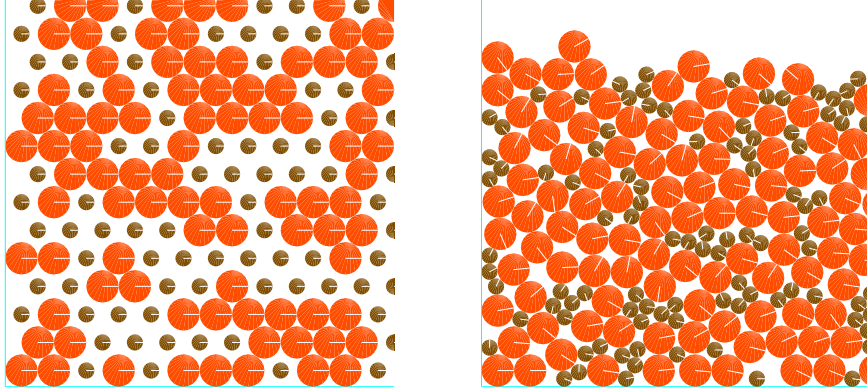


Figure 13: Example 3 – Zoom on balls falling under the gravity effect. Initial configuration on the left, final configuration on the right.

Method	Number of NLGS iterations (last time step)	Error ε_{glob} (last time step)	Maximal penetration (last time step)	Total CPU time (s)
SBP	5000	$0.119 \cdot 10^{-6}$	$0.213 \cdot 10^{-5}$	1092.95
SAL	5000	$0.135 \cdot 10^{-6}$	$0.533 \cdot 10^{-5}$	973.31
EBP	5000	$0.156 \cdot 10^{-6}$	$0.286 \cdot 10^{-6}$	854.31
EAL	5000	$0.101 \cdot 10^{-6}$	$0.390 \cdot 10^{-17}$	916.65

Table 3: Comparison of the results obtained by the four methods on the third example (after the 1000th iteration, $N_{max} = 5000$ iterations)

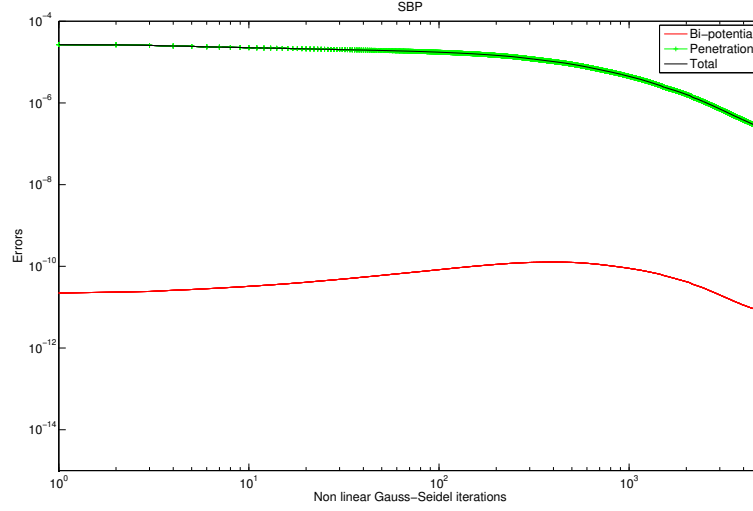


Figure 14: Example 3 – Convergence of the non-linear Gauss-Seidel iterations for the standard bi-potential based method (1000th time step). The two last curves collapse.

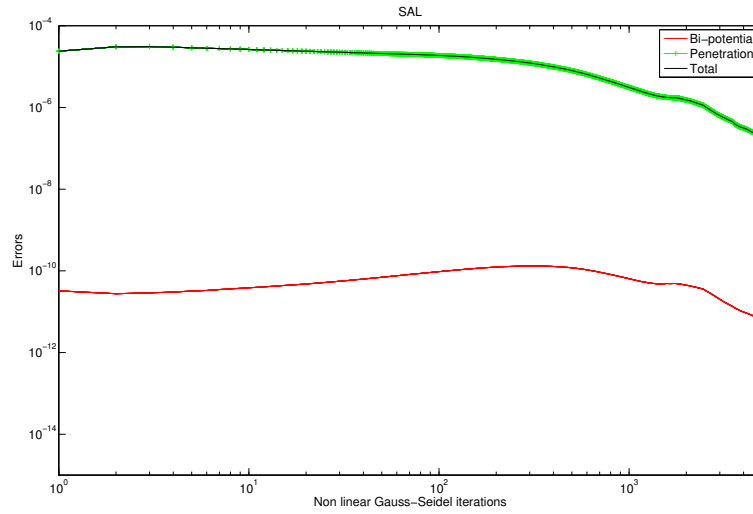


Figure 15: Example 3 – Convergence of the non-linear Gauss-Seidel iterations for the standard augmented lagrangian method (1000th time step). The two last curves collapse.

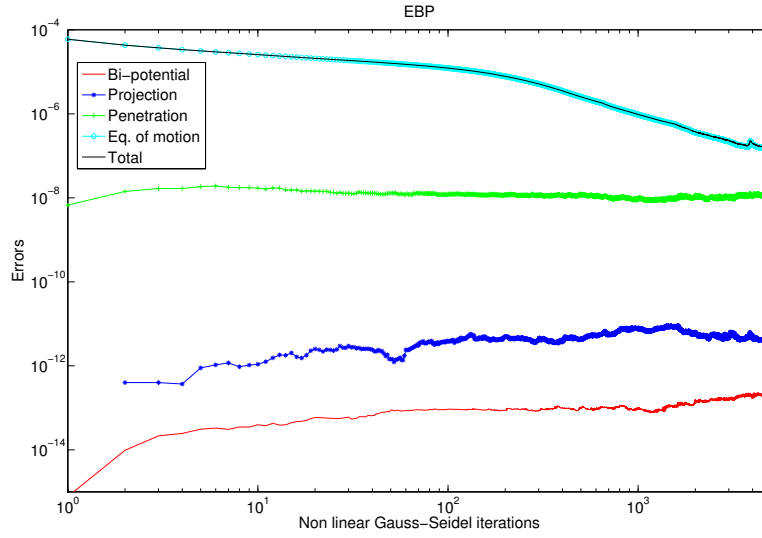


Figure 16: Example 3 – Convergence of the non-linear Gauss-Seidel iterations for the Newton and bi-potential method (1000th time step). The two last curves collapse.

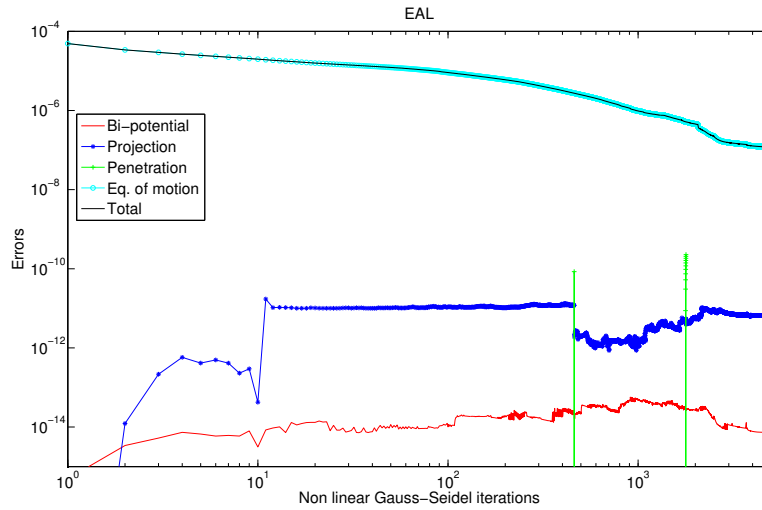


Figure 17: Example 3 – Convergence of the non-linear Gauss-Seidel iterations for the Newton and Augmented Lagrangian method (1000th time step). The two last curves collapse.

4.4 Discussion on the descent parameter ρ

We consider again the third example solved by the Newton and bi-potential method ($\varepsilon_{tot} = 10^{-8}$, maximal number of iterations of Newton method equal to 100, $\varepsilon_{Newt} = 10^{-5}$, 500th time step). Here, we take $\bar{\rho} = \frac{m_i m_j}{m_i + m_j} \frac{1}{\Delta t}$, and we consider $\rho = \alpha \bar{\rho}$, for various values of α .

α	Number of NLGS iterations (last time step)	Maximal penetration (last time step)	Total CPU time (s)
5	652	$0.110 \cdot 10^{-6}$	65.08
2	414	$0.177 \cdot 10^{-6}$	55.86
1	750	$0.149 \cdot 10^{-6}$	53.95
$\frac{1}{2}$	812	$0.634 \cdot 10^{-6}$	78.43
$\frac{1}{5}$	667	$0.219 \cdot 10^{-5}$	176.14

Table 4: Comparison of the results obtained for various values of $\rho = \alpha \bar{\rho}$ on the third example (after the 500th iteration, $N_{max} = 5000$ iterations)

These results show one of the main advantage of the EBP method. Indeed, one can notice that in table 4, the CPU time and the quality of the solution are very similar if α is equal to 1 or 2. Even if α is equal to five, the convergence is not to damaged. In that case, one remain the the SBP and the SAL are no longer convergent. If the parameter α is small, the method converges but the convergence rate is very small. One can notice that the EAL method is much more sensitive about the parameter α , essentially in the convergence of the Newton method.

5 Conclusion

The results presented show that, using an appropriate Newton method, it is possible to improve the computational time over that 20% compared to the standard methods. Moreover, one principal drawback of that type of methods, that is the dependance of the results on the parameter ρ does not exist anymore.

In the future, this method will be extended to the case of a contact law with adhesion. This improvement will be realized in a near future.

Acknowledgment: This work was supported by the french CNRS grant "PEPS Opticon-tact", and by the project "TRIBAL" supported by the Picardy region and the European funds FEDER.

References

- [1] P. Alart and A. Curnier. A mixed formulation for frictional contact problems prone to Newton like solution method. *Computer Methods in Applied Mechanics and Engineering*, 92(3):353–375, 1991.
- [2] G. De Saxcé, Z.-Q. Feng. New inequality and functional for contact with friction: the implicit standard material approach. *Mechanics of Structures and Machines*, 19:301–325, 1991.
- [3] Z.-Q. Feng, P. Joli, J.-M. Cros, B. Magnain, The bi-potential method applied to the modeling of dynamics problems with friction. *Math. Comput.*, 36:375–383 (2005).
- [4] J. Fortin, Simulation numérique de la dynamique des systèmes multicorps appliquée aux milieux granulaires. PhD Thesis (en french), University of Lille 1, 2000.
- [5] J. Fortin, M. Hjaaj, G. de Saxcé, *An improved discrete element method based on a variational formulation of the contact law*, *Computers and Geotechnics*, 29 (2002), 609–640.
- [6] J. Fortin, O. Millet, G. de Saxcé, *Numerical Simulation of Granular Materials by an improved Discrete Element Method*, *Int. J. for Num. Methods in Engineering*, no. 62, pp. 639–663, (2005).
- [7] M. Jean and J. J. Moreau. Unilaterality and dry friction in the dynamics of rigid bodies collection. In A. Curnier, editor, *Contact Mechanics International Symposium*, pages 31– 48. Presses Polytechniques et Universitaires Romanes, 1992.
- [8] M. Jean. The non smooth contact dynamics method. *Compt. Methods Appl. Math. Engrg.*, 177:235–257, 1999.
- [9] P. Joli, Z.-Q. Feng. Uzawa and Newton algorithms to solve frictional contact problems within the bi-potential framework. *Int. J. for Num. Methods in Engineering*, no. 73, pp. 317–330, (2008).
- [10] F. Jourdan, P. Alart, M. Jean. A Gauss-Seidel like algorithm to solve frictional contact problems. *Computer Methods in Applied Mechanics and Engineering*, 155:31–47 (1998).
- [11] J. J. Moreau. Unilateral contact and dry friction in finite freedom dynamics. In J.J. Moreau and eds. P.-D. Panagiotopoulos, editors, *Non Smooth Mechanics and Applications*, CISM Courses and Lectures, volume 302 (Springer-Verlag, Wien, New York), pages 1–82, 1988.
- [12] J. J. Moreau. Some numerical methods in multibody dynamics: application to granular materials. *Eur. J. Mech. A Solids*, 13(4-suppl.):93–114, 1994.

- [13] J. J. Moreau. Numerical aspect of sweeping process. *Compt. Methods Appl. Math. Engrg.*, 177:329–349, 1999.
- [14] M. Renouf and P. Alart. Conjugate gradient type algorithms for frictional multicontact problems: applications to granular materials. *Comput. Methods Appl. Mech. Engrg.*, 194(18-20):2019–2041, 2004.
- [15] M. Renouf and P. Alart. Gradient type algorithms for 2d/3d frictionless/frictional multicontact problems. In K. Majava P. Neittaanmaki, T. Rossi, O. Pironneau (eds.) R. Owen, and M. Mikkola (assoc. eds.), editors, *ECCOMAS 2004*, Jyväskylä, 24–28 July 2004.
- [16] M. Renouf, F. Dubois, and P. Alart. A parallel version of the Non Smooth Contact Dynamics algorithm applied to the simulation of granular media. *J. Comput. Appl. Math.*, 168:375–38, 2004.
- [17] M. Renouf, V. Acary, and G. Dumont. Comparison of algorithms for collisions, contact and friction in view of real-time applications. In *Multibody Dynamics 2005 proceedings*, International Conference on Advances in Computational Multibody, Madrid, 21-24 June 2005.
- [18] M. Renouf, D. Bonamy, F. Dubois, and P. Alart. Numerical simulation of two-dimensional steady granular flows in rotating drum: On surface flow rheology. *Phys. Fluids*, 17:103303, 2005.
- [19] R.T. Rockafellar. *Convex Analysis*, Vol. 28, Princeton Math. Series, Princeton Univ. Press, 1970.
- [20] N. A. Ramaniraka, *Thermomécanique des contacts entre deux solides déformables*, EPFL PhD no. 1651 (1991), Ecole Polytechnique Fédérale de Lausanne.
- [21] I. Sanni. *Modélisation et simulation bi et tri-dimensionnelles de la dynamique unilatérale des systèmes multi-corps de grandes tailles: application aux milieux granulaires*. PhD Thesis (en french), University of Picardy, 2006.